Fluorinated-PLGA Nanoparticles for Enhanced Drug Encapsulation and ^{19}F-NMR Detection

Giulia Neri,[b, a] Giuliana Mion,[a] Andrea Pizzi,[a] Wanda Celentano,[c] Linda Chaabane,[d] Michele R. Chierotti,[e] Roberto Gobetto,[e] Min Li,[f] Piergiorgio Messa,[f] Floryan De Campo,[g] Francesco Cellesi,[c] Pierangelo Metrangolo,[a] and Francesca Baldelli Bombelli*[a]

[a] Dr G. Neri, Dr G. Mion, Dr A. Pizzi; Prof. P. Metrangolo, Prof. Fr. Baldelli Bombelli
Laboratory of Supramolecular and Bio-Nanomaterials (SupraBioNanoLab), Department of Chemistry, Materials, and Chemical Engineering "Giulio Natta"
Politecnico di Milano
V. Luigi Mancinelli, 20131 Milan, Italy

E-mail: francesca.baldelli@polimi.it

[b] Dr G. Neri
Department of Chemical, Biological, Pharmaceutical and Environmental Sciences
University of Messina
V.le F. Stagno d'Alcontres, 31, 98166 Messina, Italy

[c] Dr W. Celentano, Prof. Fr. Cellesi
Department of Chemistry, Materials, and Chemical Engineering "Giulio Natta"
Politecnico di Milano
V. Luigi Mancinelli, 20131 Milan, Italy

[d] Dr L. Chaabane
Institute of Experimental Neurology (INSPE) and Experimental Imaging Center (CIS)
IRCCS San Raffaele Hospital
V. Olgettina, 60, 20132 Milan, Italy

[e] Prof. M. Chierotti, Prof. R. Gobetto
Department of Chemistry and NIS Centre
Università di Torino
V. Pietro Giuria, 7, 10125 Turin, Italy

[f] Dr M. Lin, Prof. P. Messa
Renal Research Laboratory
Fondazione IRCCS Ca' Granda Ospedale Maggiore Policlinico
V. Francesco Sforza, 35 20122 Milan, Italy

[g] Dr Fl. De Campo
Solvay Specialty Polymers
V. Lombardia, 20, Bollate, 20021 Milan, Italy

Abstract: In the continuous search to develop multimodal systems with combined diagnostic and therapeutic functions, several efforts have been focused on the development of multifunctional drug delivery systems. Herein we designed, by a covalent approach, a novel class of fluorinated poly(lactic-co-glycolic acid) co-polymers (F-PLGA) containing an increasing number of magnetically equivalent fluorine atoms. In particular, two novel compounds, F_3-PLGA and F_9-PLGA, were synthesized and their chemical structure and thermal stability were analysed by solution NMR, DSC, and TGA. The obtained F-PLGA compounds were proved to form in aqueous solution colloidal stable nanoparticles (NPs) displaying a strong ^{19}F-NMR signal. The fluorinated NPs also showed an enhanced ability to load hydrophobic drugs containing fluorine atoms with respect to analogue pristine PLGA NPs. Preliminary *in vitro* studies showed their cellular availability and ability to intracellularly deliver and release a functioning drug.

Introduction

Over the last few decades, multimodal polymer nanoparticles (NPs) have been extensively investigated in medicine with the objective of combining diagnostic and therapeutic functions in the same particle.[1] The FDA-approved poly(lactic-co-glycolic acid) co-polymer (PLGA) is among the most attractive polymeric material for biomedical applications, thanks to its high biocompatibility and biodegradability, long-term storage stability, and ability to encapsulate and protect drugs by *in vivo* fast degradation.[2] In fact, time releases of the encapsulated cargoes from NPs can be fine-tuned by modulating polymer composition and structural modifications.[3]

In last decades, several multimodal PLGA NPs have been developed through their combination with various imaging techniques, such as magnetic resonance imaging (MRI),[4] ultrasound (US),[5] and optical imaging (OI).[6] Among available non-invasive imaging techniques, the potential of ^{19}F-MRI has recently emerged thanks to the high natural abundance of the ^{19}F nucleus, its high gyromagnetic ratio, and its null *in vivo* detectable background due to the extremely low concentration of fluorine in living systems.[7] This results in a high specificity of

^{19}F-MRI with the possibility to directly quantify the signal and the amount of ^{19}F by imaging,[8] with a promising use of ^{19}F probes for *in vivo* cell tracking.[9] Ideal requirement for highly sensitive ^{19}F-MRI probes for clinical use is being biocompatible and bearing a high number of magnetically equivalent ^{19}F atoms. Additionally, fluorination is a chemical modification often used in pharmaceutics to change drug properties such as metabolic stability, lipophilicity and bioavability, in fact about 30% of new drugs contains at least an atom of fluorine.[10] Hence ^{19}F-NMR has been widely used as selective method to detect and quantify fluorinated pharmaceutics. Fluorinated residues, beyond reducing water solubility, are known to generally avoid interactions with other elements through the so-called fluorophobic effect.[11] In this context, it has been recently showed that fluorination of hydrophobic pockets forming a confined space within gold supraparticles enhanced their encapsulation efficiency of poorly soluble drugs containing fluorine atoms.[12]

For these reasons, covalent functionalization of biocompatible materials with suitable fluorinated ligands[13] can be an interesting strategy to produce efficient drug nanocarriers also detectable by ^{19}F-NMR.[14] Critical to the development of an effective ^{19}F-NMR probe is to facilitate the mobility of the fluorinated chains, in order to achieve the necessary transverse relaxation time (T_2) for a good signal image.[15] In this sense, the use of short and branched fluorinated ligands is preferable to the counterpart linear chains, also in terms of biodistribution and bioaccumulation.[7b, 16]

Here, we report a covalent strategy to directly functionalize PLGA with a highly mobile fluorinated group to be active in ^{19}F-NMR without impacting its self-assembly ability. A PLGA co-polymer has been functionalized with two different fluorinated amine ligands, which contain three and nine equivalent fluorine atoms, respectively. Thus, two novel compounds, F_3-PLGA and F_9-PLGA, for which synthesis and chemical structure are reported in Scheme 1, were obtained. Their chemical structure and thermal stability were analysed by solution NMR, DSC, and TGA. Moreover, the ability of F_9-PLGA NPs to function as both ^{19}F-NMR probes and drug carriers was also investigated. At this stage, we selected the drugs based on their structural properties to systematically investigate the encapsulation of fluorinated drugs in the fluorinated polymer. In this sense, intrinsic ability of PLGA NPs to encapsulate hydrophobic molecules and concomitant presence of fluorinated groups in the confined space of F-PLGA NPs were considered important parameters. Thus, two hydrophobic drugs with different number of ^{19}F atoms were selected as drug models: Dexamethasone (DEX), a synthetic steroidal anti-inflammatory drug containing one fluorine atom,[17] and leflunomide (LEF), an immunosuppressive disease-modifying antirheumatic drug (DMARD) containing three fluorine atoms.[18] Structural organization and morphology of the NPs were elucidated by DLS, solid-state NMR, and TEM analysis. To evaluate eventual cytotoxicity of the F-PLGA NPs, preliminary *in vitro* tests on kidney glomerular cells were also performed. Finally, podocyte repair due to a controlled intracellular delivery of DEX from F_9-PLGA NPs was also demonstrated to show the efficacy of the released drug.

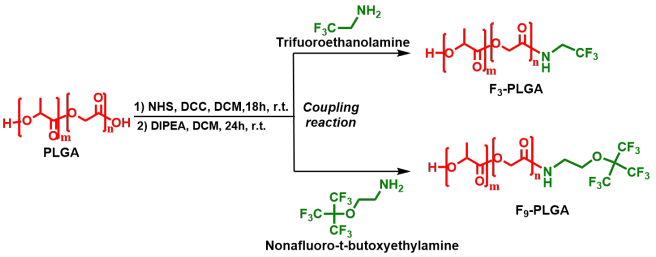

Scheme 1. Synthesis and chemical structures of the fluorinated PLGA (F-PLGA) derivatives: F_3-PLGA and F_9-PLGA.

Results and Discussion

PLGA was purified and functionalized with two different fluorinated molecules *via* amide-coupling reactions with a slight modification with respect to the procedure reported in literature.[19] After PLGA activation by *N*-Hydroxysuccinimide (NHS), the intermediate was covalently conjugated using *N*,*N*-diisopropylethylamine (DIPEA) to either trifluoroethanolamine or nonafluoro-*t*-butoxyethylamine HCl, with the production of two new fluorinated polymers, F_3-PLGA and F_9-PLGA (Scheme 1), containing three and nine magnetically equivalent ^{19}F atoms, respectively (see "Experimental Section" section for the detailed synthetic procedure).

Molecular number (Mn), molecular weight (Mw), and dispersity (Đ) values relative to PLGA, F_3-PLGA, and F_9-PLGA were evaluated by GPC analysis (Table S1). Moreover, the thermal stabilities of purified PLGA (PLGA), F_3-PLGA, and F_9-PLGA were estimated by TGA and DSC analyses. Thermogravimetric (TG) curves of all the samples were characterized by one main mass loss step with an increase of thermal stability upon fluorination and a starting degradation point at around 200 °C (Figure S1 and Table S2). DSC curves showed glass transition (Gl. Tr.) events between 30°- 47° C (Table S2), with no melting point for all the samples, indicating their amorphous nature, in agreement with the literature.[20]

PLGA, F_3-PLGA and F_9-PLGA NPs were formulated by nanoprecipitation method in surfactant free conditions (see Figure 1 and the "Experimental Section" section for the formulation details) using a 1:1 acetone-water volume ratio with a final pH=6.4.

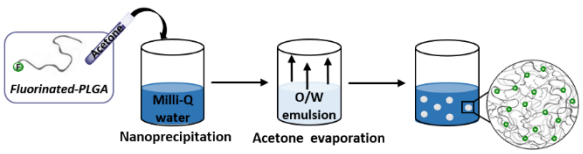

Figure 1. Schematic representation of nanoprecipitation method for the formulation of F-PLGA NPs.

The obtained NPs were characterized by DLS, TEM, and ^{19}F-NMR techniques. DLS analysis of PLGA, F_3-PLGA, and F_9-PLGA NP dispersions showed that they were characterized by average hydrodynamic radii (R_H) of 61 ± 5 nm (Table S3), 54 ± 6 nm (Figure 2B, Table S3), and 58 ± 6 nm (Figure 2E, Table S3),

respectively, with good polydispersity indexes (PDI) (Table S3). The intensity-weighted <R_H> size distribution evaluated by CONTIN analysis was in agreement with TEM size distribution for both fluorinated samples (Figures 2A and 2D). More importantly, a characteristic sharp ^{19}F-NMR signal at around -72 ppm and -70 ppm was recognized for F_3-PLGA NPs (Figure 2C) and F_9-PLGA NPs (Figure 2F), respectively, indicating that self-assembly did not impair the mobility of the fluorinated chains.

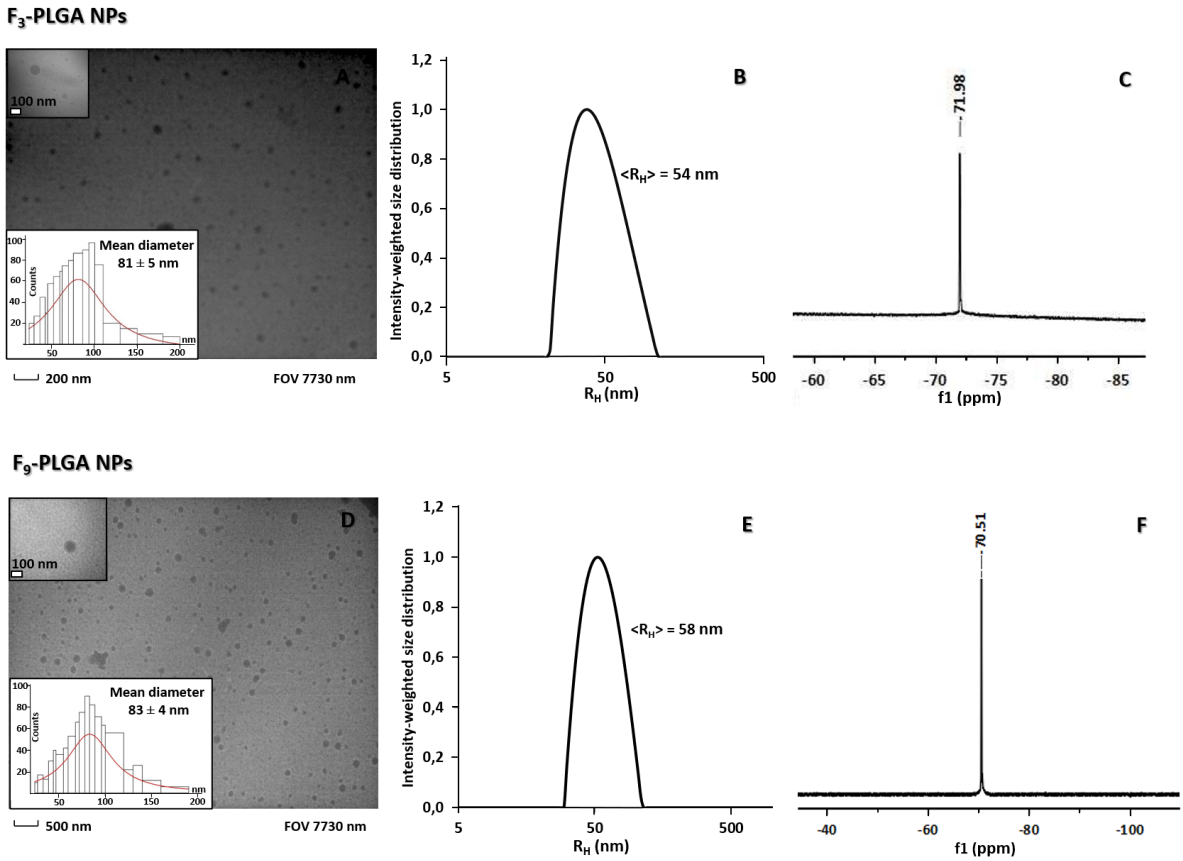

Figure 2. TEM images of a dispersion of F_3-PLGA NPs (**A**) and of F_9-PLGA (**D**), respectively. The distribution size of both F_3-PLGA NP (**B**) and F_9-PLGA NP (**E**) dispersions was confirmed by DLS analysis. The DLS data were obtained at the same NP concentration 10 mg/mL. ^{19}F-NMR (400 MHz) spectra show the characteristic ^{19}F signals of F_3-PLGA NPs (**C**) and of F_9-PLGA NPs (**F**).

Moreover, in order to evaluate the efficiency of F_3-PLGA NPs and F_9-PLGA NPs as ^{19}F-NMR probes, their longitudinal (T_1) and transverse (T_2) relaxation times were evaluated. F_3-PLGA NPs and F_9-PLGA NPs showed T_1 values of 537 ms and 625 ms and T_2 values of 122 ms and 60 ms, respectively, in agreement with values found for other ^{19}F-MRI active NP systems,[21] indicating their suitability for ^{19}F-MRI applications.[22] As expected, the increase of ^{19}F atoms in the molecular structure significantly raised the intensity of the ^{19}F-NMR signal of F_9-PLGA NPs with respect to that of F_3-PLGA NPs. This was proved performing the ^{19}F-NMR analysis on F_3-PLGA and F_9-PLGA NP dispersions at the same polymer concentration in presence of trifluoroacetic acid (TFA) standard solution (Figure S2). Therefore, further characterizations were focused on the most promising F_9-PLGA NPs.

The efficiency of F_9-PLGA NPs as drug carriers was proven by testing their ability to encapsulate two different hydrophobic drugs containing ^{19}F atoms: Dexamethasone (DEX) with one ^{19}F atom, and leflunomide (LEF) with three ^{19}F atoms. The hydrophobic nature of these drugs is demonstrated by their logP values: ~1.68 (polar surface area, PSA, 94.83 Å^2) for DEX and ~2.52, (PSA 55.10 Å^2) for LEF. Drug-loaded PLGA and F_9-PLGA NPs were formulated using the same acetone-water emulsion method used for drug-free NPs,[23] adding the drug to the organic solution (see "Experimental Section" section for the detailed synthetic procedure). The encapsulation process was optimized at a constant 1:10 polymer:drug weight ratio for the two different drugs for PLGA and F_9-PLGA, obtaining DEX@F_9-PLGA/PLGA and LEF@F_9-PLGA/PLGA NPs (detailed procedure in the Experimental Section).

First, morphology of the drug loaded NPs was investigated by DLS and TEM analysis. TEM analysis did not show significant changes in morphology and size with respect to unloaded NPs and obtained size distributions were characterized by mean diameters of 83 ± 5 nm (DEX@F_9-PLGA, Figure S3A) and 91 ± 5 nm (LEF@F_9-PLGA, Figure S3B). DLS results showed quite similar averaged hydrodynamic sizes and PDI values for loaded and unloaded NPs (Table 1). DEX and LEF loading was first qualitatively evaluated by ATR-FTIR analysis to detect the characteristic signal of the drugs (Figures S4 and S5), while quantitative amounts of the entrapped drug within the NPs were determined by HPLC analysis (see "Experimental Section" for the experimental details) calculating drug loading capacity %

(DL%) and encapsulation efficiency % (EE%) of the F_9-PLGA NPs with respect to pristine PLGA NPs in the same conditions.
Considering both encapsulation efficiency (EE%) and drug loading capacity (DL%) results, two observations can be made: F_9-PLGA NPs encapsulated a higher amount of drug (DEX/LEF) with respect to the unmodified PLGA and both F_9-PLGA and PLGA NPs showed higher values of EE% and DL% for LEF than for DEX. Moreover, both drug loaded nanoformulations exhibited a strong ^{19}F signal at – 70.5 ppm (Figure S6A). In addition, the ^{19}F signal of the -CF_3 group of LEF at around -62 ppm was also recognized in the spectrum of LEF@F_9-PLGA NPs (Figure S6B) thanks to the higher number of fluorine atoms in the chemical formula as well as its higher loading. The detection of LEF by ^{19}F-NMR with a specific chemical shift different from that of the polymer it is quite important, as it might allow the simultaneous tracking of both drug and carrier. While T_1 values are quite promising, a decrease of the T_2 values for both DEX@F_9-PLGA_NPs and LEF@F_9-PLGA_NPs with respect to the starting unloaded F_9-PLGA_NPs (Table S4) was observed, indicating a lower mobility of the fluorinated chains upon drug loading. However, resulting T2 values are still higher than those of other drug loaded fluorinated polymer NPs.[13c]

Table 1. DLS data relative to PLGA and F_9-PLGA NPs are reported. DLS, DL%, and LL% data relative to DEX@F_9-PLGA and to LEF@F_9-PLGA NPs

	PLGA NPs	F_9-PLGA NPs	DEX@ PLGA	DEX@ F_9-PLGA	LEF@ PLGA	LEF@ F_9-PLGA
$<R_H>$ (nm) [a]	61±5	58±6	74±5	64±5	75±5	63±6
PDI[b]	0.14	0.15	0.10	0.15	0.23	0.16
DL%[c]	-	-	2.1 ±0.3	4.2 ±0.3	6.3 ±1.5	9.3 ±2.4
EE%[d]	-	-	16.5 ±3.5	29.5 ±2.1	59.0 ± 10.0	78.5 ±10.0

formulated at 1:10 and drug: polymer weight ratio are reported.

[a] Hydrodynamic radius. [b] Polydispersity index. [c] Drug loading capacity%. [d] Encapsulation efficiency%.

Moreover, it has been shown for other systems that it is possible to have an intracellular raise in T2 upon drug release.[24]
A combination of two different effects seems to govern the drug encapsulation process: First, considering the common attitude of PLGA to entrap highly hydrophobic molecules, it is reasonable that both F_9-PLGA and PLGA NPs encapsulated a higher amount of more hydrophobic LEF. Higher encapsulation yields observed for F_9-PLGA NPs with respect to unmodified PLGA NPs might be explained by an increased fluorophilicity of the confined environment (*i.e.*, possible F-F interactions among the fluorinated groups of the polymer and the drugs).[12] The hypothesis of possible F-F interactions was investigated through solid-state NMR on lyophilized LEF@F_9-PLGA NP formulations. In Figures S7 and S8 are reported the ^1H-^{13}C and ^{19}F-^{13}C CPMAS NMR spectra of LEF@F_9-PLGA NPs, F_9-PLGA NPs and pure LEF. The ^1H-^{13}C CPMAS NMR spectrum of LEF@F_9-PLGA NPs shows the presence of the drug in the lyophilized NPs according to its weight percentage (about 7%). This agrees with the ^{19}F MAS SSNMR spectrum (Figure S9 in comparison with those of pure LEF and F_9-PLGA), which is characterized by two different resonances (-60.7 and -59.5 ppm) for the LEF molecule loaded into the NPs. The presence of two signals indicates two different chemical environments for LEF in the NPs, in agreement with the broad ^{13}C resonance observed in the ^{19}F-^{13}C CPMAS spectrum (Figure S8). Moreover, 2D ^{19}F DQ MAS experiments were performed to highlight correlations due to pairs of through-space dipolar coupled fluorine atoms, *i.e.*, close in space fluorine atoms. In general, they are able to probe possible LEF-F_9-PLGA NPs CF_3 intermolecular interactions, thus providing insights on the LEF distribution inside the nanoparticles. The 2D ^{19}F DQ MAS spectrum of LEF@F_9-PLGA NPs (Figure S10) does not show any correlation either between two LEF sites (-60.7 and -59.5) either between LEF sites and CF_3 groups of the F_9-PLGA NPs. These results demonstrated that drug encapsulation process was not enhanced by occurrence of direct and cooperative intermolecular F-F drug-polymer interactions, but it was probably due to a general increased attitude of the hydrophobic drugs to the fluorinated environment within the NP.
At this stage to finally prove the ability of these NPs to deliver and release the encapsulated drug intracellularly, we selected DEX@loaded NPs due to the possibility to easily monitor the functionality of the drug through an already optimized bioassay. PLGA and F_9-PLGA NPs loaded with DEX were assessed in terms of *in vitro* cytotoxicity on immortalized human glomerular endothelial cells (HCiGEnC) and podocytes (HCiPodo), taking into account the constant interaction of the NPs during *in vivo* blood circulation with the cells of the kidney glomerular filtration barrier.[25] Cells were cultured at 37 °C in presence of different concentrations of NPs (0.01–2 mg/mL) for 24 h. Lactate Dehydrogenase (LDH) colorimetric assay was selected for the test as it was proven to be an efficient indicator of cytotoxicity for kidney glomerular cells.[25b, 26] PLGA and F_9-PLGA, with and without loaded DEX, showed negligible cytotoxicity on both cell lines up to a concentration of 2 mg/mL (Figure 3A and 3B), which confirmed the high biocompatibility of the polymeric nanomaterials even when fluorinated and drug-loaded. The therapeutic effect of DEX-loaded F_9-PLGA NPs was also assessed on damaged podocytes *in vitro*. Alteration of their cytoskeleton morphology is known to be a good indicator of pathological condition in chronic kidney diseases,[25b, 27] therefore the efficacy of DEX@F_9-PLGA NPs on these cells was assessed by evaluating F-actin orientation on HCiPodo cells, before and after the treatment.[25b, 26] Cell damage was induced with Adriamycin (ADR) incubation for 24 h, as confirmed by the reduced density and irregular distribution of the actin fibres (green-phalloidin staining), together with a disappearance of cell protrusions (Figure 3C). After 48 h of incubation with the NPs, podocytes displayed a more regular distribution of F-actin along the whole cell body and processes, which indicated a recovered healthy morphology (Figure 3D). These results demonstrated that DEX bioactivity was retained during the particle manufacturing process

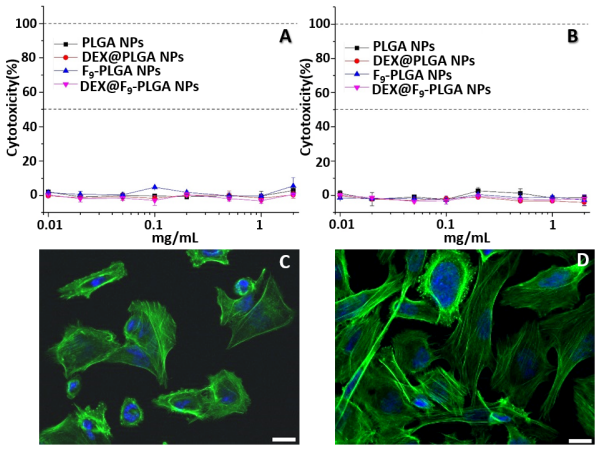

Figure 3. LDH assay on HCiGEnC (A) and HCiPodo cells (B) incubated with NPs (PLGA, DEX@PLGA, F_9-PLGA, DEX@F_9-PLGA) for 24 h, at concentrations from 0.01 to 2 mg/mL. Y-axis: Normalised Cytotoxicity = (Test sample-Low control) / (High control-Low control); Low control: normal cells; High control: cells treated with lysis buffer C) HCiPodo cells (stained by green phalloidin and DAPI, scale bar 20 μm) were treated with ADR to induce podocyte damage in vitro. D) Effect of DEX@F_9-PLGA (DEX concentration 10μM) incubated with ADR-damaged HCiPodo cells for 48 h; cells recovered the normal orientation of actin stress fibers.

Conclusions

In conclusion, synthesis, characterization, and formulation of two new fluorinated PLGA nanocarriers, F_3-PLGA and F_9-PLGA, were reported. F_9-PLGA NPs were found more promising in terms of ^{19}F-NMR signal. The drug loading process did not impair their ^{19}F-NMR activity of F_9-PLGA NPs, while higher ability to encapsulate hydrophobic drugs compared to unmodified PLGA NPs was observed. Moreover, F_9-PLGA NPs loaded with DEX were applied on immortalized human glomerular endothelial cells (HCiGEnC) and podocytes (HCiPodo) at different concentrations, showing no cytotoxicity. The efficacy of F_9-PLGA NPs to release bioactive DEX on damaged podocytes was also proved, showing a recovered healthy morphology of these cells after 48 h incubation with the loaded NPs. Taking in account these preliminary results, we believe that F_9-PLGA NPs could be an optimal candidate as multifunctional drug delivery system.

Experimental Section

Materials

N–Hydroxysuccinimide ($C_4H_5NO_3$), *N,N'*-Dicyclohexylcarbodiimide ($C_{13}H_{22}N_2$), *N,N*- diisopropylethylamine ($[(CH_3)_2CH]_2NC_2H_5$), Acryloyl chloride (C_3H_3OCl), Triethylamine ($C_6H_{15}N$), Tris(2-carboxyethyl)phosphine hydrochloride ($C_9H_{15}O_6P$ HCl), Methyl Iodide (CH_3I), Sodium Hydride (NaH), and Dexamethasone ($C_{22}H_{29}FO_5$) were purchased from Sigma Aldrich. 2,2,2- Trifluoroethanolamine ($C_2H_4NF_3$), Nonafluoro-*t*-butoxyethylamine · HCl ($C_6H_7ClF_9NO$), and 3,3,3-Trifluoropropylmercaptan ($C_3H_5F_3S$), Trifluoroacetic acid ($C_2HF_3O_2$) were purchased from FluoroChem. Leflunomide ($C_{12}H_9F_3N_2O_2$) was purchased from TCI Europe N.V. PLGA (LA:GA= 50:50, Mn ~ 4732) was provided by Solvay Specialty Polymers.

Synthesis of ((2,2,2-trifluoroethyl)amide-terminated poly(-lactide–co–glycolide) (F_3-PLGA)

In order to increase the purity of PLGA starting material, it was precipitated in cold Et_2O. Then, PLGA (0.33 mmol, 1 eq) was dissolved in 10 mL of anhydrous CH_2Cl_2 and converted to PLGA-NHS with an excess of *N*-Hydroxysuccinimide (NHS) (1.32 mmol, 4 eq) in presence of *N,N'*-Dicyclohexylcarbodiimide (DCC) (1.38 mmol, 4.2 eq), which was added at 0 °C. Then, the solution became cloudy and it was left stirring at r.t. overnight. The solid urea-DCC was removed by centrifugation treatment. Afterwards, the obtained supernatant was filtered (0.2 μm PTFE syringe filter) to remove any trace of insoluble solid urea-DCC by product. To remove residual NHS unreacted, PLGA-NHS was precipitated from CH_2Cl_2 solution with cold Et_2O, and washed several times Et_2O. The precipitate was dried under vacuum at 50° C and a white solid was obtained.

PLGA-NHS (0.33 mmol, 1 eq) was dissolved in 6 mL of anhydrous CH_2Cl_2, then 2,2,2-trifluoroethanolamine (1.27 mmol, 3.86 eq) and *N,N*-diisopropylethylamine (DIPEA) (1.43 mmol, 4.34 eq), with a slight modification with respect to the procedure reported in the literature,[19] were added. The solution was left stirring overnight at r.t. under N_2 atmosphere. Then, the solution was concentrated under vacuum and the product was precipitated with cold Et_2O. In order to increase the purity of F_3-PLGA, it was washed several times with MQ Water and dried under vacuum at 50° C. ^{1}H-NMR (400 MHz, $CDCl_3$, δ, ppm): 6.86-6.55 (brs, O*H*), 5.26-5.18 (m, 1H, C*H* PLGA), 4.89-4.67 (m, 2H CH_2 PLGA), 3.95 (m, 2H, CH_2), 1.58-1.59 (d, 3H, CH_3 PLGA). ^{13}C-NMR (400 MHz, $CDCl_3$, δ, ppm): 169.49, 166.43, 69.25, 60.88, 40.30, 16.66. ^{19}F-NMR (400 MHz, $CDCl_3$, δ, ppm): -72.49 (s, 3F, CF_3).

Synthesis of ((2-((1,1,1,3,3,3-hexafluoro-2(trifluoromethyl)propan-2-yl)oxy)ethyl)amide-terminated poly(-lactide–co–glycolide), (F_9-PLGA)

The PLGA-NHS was obtained as previously reported in the F_3-PLGA synthetic strategy. PLGA-NHS (0.33 mmol, 1 eq) was dissolved in 6 mL of anhydrous CH_2Cl_2, then nonafluoro-*t*-butoxyethylamine HCl (0.28 mmol, 1 eq) and *N,N*-diisopropylethylamine (DIPEA) (1.15 mmol, 4 eq) were added [19]. The solution was left stirring overnight at r.t. in N_2 atmosphere. Subsequently, the solution was concentrated and F_9-PLGA was precipitated with cold Et_2O. In order to increase the purity of the product, F_9-PLGA was washed with Brine solution and dried under vacuum at 50 °C. ^{1}H-NMR (400 MHz, $CDCl_3$, δ, ppm): 6.61 (brs, O*H*), 5.26-5.19 (m, 1H, C*H* PLGA), 4.88-4.60 (m, 2H, CH_2 PLGA), 4.12 (m, 2H, CH_2), 3.59 (m, 2H, CH_2), 1.57-1.59 (d, 3H, CH_3). ^{13}C-NMR (400 MHz, CDCl3, δ, ppm): 169.52, 166.46, 69.29, 68.54, 60.90, 38.99, 16.69. ^{19}F-NMR (400 MHz, CDCl3, δ, ppm): -70.37 (s, 9F, CF_3).

Preparation of PLGA NPs

NPs were formulated by nanoprecipitation method in surfactant free conditions using 1:1 acetone-water volume ratio with a final pH=6.4. The procedure consists of the drop-wise addition of 1 mL (~ 2 min) of either purified PLGA or F-PLGA 10 mg/mL solution in acetone to a 1 mL of MQ Water. The obtained emulsion was left stirring for 15 min and the organic solvent was fully removed under vacuum and checked by ^{1}H-NMR using deuterated acetone.

NP Drug Loading

Dexamethasone and leflunomide were solubilized in acetone to prepare two solutions of 1 mg/mL and 2 mg/mL concentration, respectively. Then 10 mg of polymer (PLGA or F_9-PLGA) were solubilized in 1 mL of dexamethasone solution and 20 mg of polymer (PLGA or F_9-PLGA) were solubilized in 1 mL of leflunomide solution. Then, each mixture was drop-wise added to 1 mL of MQ Water and the suspension was stirred for 15 min at 25 °C. The dispersion was centrifuged to remove the unloaded drug. Afterwards, the acetone was removed under vacuum and checked by ^{1}H-NMR using deuterated acetone; then the NPs were lyophilized.[28]

Dexamethasone (DEX) and leflunomide (LEF) contents were determined by HPLC analyses. The lyophilized powder was dissolved in 1 mL of acetonitrile. Then, it was 1:10 diluted with acetonitrile. Each sample was injected (10 µL) in a C18 reversed-phase chromatography column at 30 °C with a flow rate of 1 mL/min in a solution of acetonitrile-water 1:1. The DEX peak was detected after ~3 min and LEF peak after ~10 min. The detection wavelength was set at 254 nm. Calibration curves were previously obtained with different DEX and LEF concentrations (1, 0.5, 0.1, 0.01, 0.001 mg/mL). Drug Loading (DL%) and Encapsulation Efficiency (EE%) values associated to each polymer were calculated according to the following equations:[29] DL%=100*(Weight of Drug Encapsulated)/ (Weight of Drug Encapsulated+ Weight of Polymer Nanoparticles)

EE%=100*(Weight of Drug Encapsulated in Polymer Nanoparticles)/ (Weight of Drug Used in Encapsulation Method).

Methods

Dynamic Light Scattering (DLS) measurements were performed on an ALV apparatus equipped with ALV- 5000/EPP Correlator, special optical fiber detector and ALV/CGS-3 Compact goniometer. The light source is He-Ne laser (λ = 633 nm), 22 mW output power. Measurements were performed at 25 °C. Approximately 1 mL of sample solution was transferred into the cylindrical Hellma scattering cell. Data analysis has been performed according to standard procedures and auto-correlation functions were analyzed through a constrained regularization method (Laplace inversion of the time auto-correlation functions), CONTIN, for obtaining the particle size distribution.

Transmission Electron Microscopy (TEM) images were acquired by using a Delong America LVEM5 microscope, equipped with a field emission gun and operating at 5 kV. Samples were prepared by dropping NP dispersions (0.3 mg/mL and 3 mg/mL) on carbon-coated copper grids and letting them dry overnight. TEM image analysis was performed using ImageJ software. Statistical analysis was based on the measurement of about 1000-4000 NPs. Size distributions were fitted by a Lorentz equation using IgorPro 4.02.

^{1}H, ^{13}C, and ^{19}F Nuclear Magnetic Resonance (NMR) spectra were performed at r. t. on a Bruker AV400 spectrometer. Chemical shifts are reported in parts per million (ppm). Multiplicities are reported as follows: s (singlet), brs (broad singlet), d (doublet), m (multiplet). Trifluoroacetic acid (TFA) was added as external standard, with chemical shift set at ~ -75.48 ppm. The ^{19}F-NMR spectra of both F_3 PLGA and F_9-PLGA NP dispersions, in presence of TFA standard solution, were collected at the same experimental condition. ^{19}F T_1 and T_2 measurements were recorded at 305 K on a Bruker AV400 spectrometer operating at 400 MHz for the ^{1}H nucleus. The inversion recovery and the CPMG pulse sequences were used for the measures of T_1 and T_2, respectively.

High Performance Liquid Chromatography (HPLC) measurements were performed on a JASCO® HPLC equipped with: 2057 autosampler; RI-2031 refraction index detector; UV-Vis detector, CO-2060 plus oven column; PU-2080 pump; MD-2018 photodiode array PDA detector; C18 column (5 µm particle size) 150 mm·4.6 mm (length × diameter), mobile phase consisted of 50/50 (v/v) water/acetonitrile. Evaluation of the drug concentration was done using the UV-Vis detector. The DEX peak was detected after ~3 min and LEF peak after ~10 min. The detection wavelength was set at 254 nm. Calibration curves were previously obtained with different DEX and LEF concentrations (1, 0.5, 0.1, 0.01, 0.001 mg/mL).

LDH Cytotoxicity. NP cytotoxicity was measured using LDH-Cytotoxicity Colorimetric Assay Kit (BioVision Inc.). Briefly, 8000 per well of conditionally immortalized human podocytes (HCiPodo) or conditionally immortalized human glomerular endothelial cells (HCiGEnC) (both from University of Bristol, Bristol, UK) were plated on a 96-well plate and cultured at 37 °C, respectively, in RPMI-1640 with 10% foetal calf serum (FCS), 5 µg/mL transferrin, 5 ng/mL sodium selenite, 0.12 U/mL insulin, 100 U/mL penicillin, 100 mg/mL streptomycin, and in EGM2-MV medium containing FCS (5%) and growth factors as supplied (Lonza, Walkersville, MD, USA), for 3-4 days. Then, the culture medium was replaced by medium containing different concentrations of NPs (0.01-2 mg/mL), which was incubated with cells for 24 hours. For positive control (high control), 10 µL of cell Lysis solution was added and incubated for 24 hours, while the low control was referred to cells incubated only with standard medium. At the end of incubation, the plate was gently shaked for some minutes and centrifuged at 600 x g for 10 min. 10 µL of culture medium from each well was transferred into a new optically clear 96-well plate, and 100 µL of LDH Reaction Mix was added to each well and incubated at room temperature for 30 min. The absorbance of all controls and samples was measured with 450 nm filter using SAFAS Spectrophotometry (Monaco). The cytotoxicity was calculated using the equation: Normalised Cytotoxicity = (Test sample-Low control)/ (High control-Low control); Low control: normal cells; High control : cells treated with lysis buffer.

Fluorescence Microscopy Examination. HciPodo and HCiGEnC were cultured on coverslips and fixed with 4% of paraformaldehyde at room temperature for 10 min. After washing, cells were treated with 0.3% of Triton in PBS for 5 min and incubated with 1% of bovine serum albumin in PBS at r.t. for 30 min. Phalloidin-FITC at 1:100 dilution, together with DAPI at 1:1000 dilution was added, and the cells were incubated for 1 h. After 3 times washing with PBS, the cells were mounted with Fluorsave aqueous mounting medium (Merck, Milano, Italy). Images were acquired using a Zeiss AxioObserver microscope equipped with a high resolution digital videocamera (AxioCam, Zeiss) and an Apotome system for structured illumination, and recorded by the AxioVision software, version 4.8.

DEX Release on Podocytes. HciPodo were plated on a 35 mm Petri dish containing four cell culture coverslips and cultured at 37 °C for 3−4 days. Afterwards, cells were incubated with 0.8 µM Adriamycin (ADR, Sigma-Aldrich) in cell culture medium for 24 h. After 24h incubation, ADR was replaced by fresh medium (as the control group) or medium with a different concentration of NPs loaded with Dexamethasone (100 µM or 10 µM) and incubated for another 24 or 48 h. Cells were finally washed thrice with PBS and characterized by fluorescence microscopy as described above.

Acknowledgements

We thank Solvay Specialty Polymers for supporting and funding this research project.

Keywords: fluorine, nanoparticles, drug delivery, nanomedicine

[1] G. Chen, I. Roy, C. Yang, P. N. Prasad, *Chemical Reviews* **2016**, *116*, 2826-2885.

[2] [a]S. Lal, A. Perwez, M. A. Rizvi, M. Datta, *Applied Clay Science* **2017**, *147*, 69-79; [b]G. Calderó, C. Fornaguera, L. Zadoina, A. Dols-Perez, C. Solans, *Colloids and Surfaces B: Biointerfaces* **2017**, *160*, 535-542; [c]B. Baghaei, M. R. Saeb, S. H. Jafari, H. A. Khonakdar, B. Rezaee, V. Goodarzi, Y. Mohammadi, *Journal of Applied Polymer Science* **2017**, *134*, 45145; [d]B. Sivakumar, R. G. Aswathy, R. Romero-Aburto, T. Mitcham, K. A. Mitchel, Y. Nagaoka, R. R. Bouchard, P. M. Ajayan, T. Maekawa, D. N. Sakthikumar, *Biomaterials Science* **2017**, *5*, 432-443.

[3] Y. Xu, C.-S. Kim, D. M. Saylor, D. Koo, *Journal of Biomedical Materials Research Part B: Applied Biomaterials* **2017**, *105*, 1692-1716.

[4] S.-J. Lee, H.-J. Kim, Y.-M. Huh, I. W. Kim, J. H. Jeong, J.-C. Kim, J.-D. Kim, *Journal of Nanoscience and Nanotechnology* **2018**, *18*, 1542-1547.

[5] Y. Li, M. Wu, N. Zhang, C. Tang, P. Jiang, X. Liu, F. Yan, H. Zheng, *Journal of Cellular and Molecular Medicine* **2018**, *22*, 4171-4182.

[6] E. R. Swy, A. S. Schwartz-Duval, D. D. Shuboni, M. T. Latourette, C. L. Mallet, M. Parys, D. P. Cormode, E. M. Shapiro, *Nanoscale* **2014**, *6*, 13104-13112.

[7] [a]I. Tirotta, V. Dichiarante, C. Pigliacelli, G. Cavallo, G. Terraneo, F. B. Bombelli, P. Metrangolo, G. Resnati, *Chemical Reviews* **2015**, *115*, 1106-1129; [b]I. Tirotta, A. Mastropietro, C. Cordiglieri, L. Gazzera, F. Baggi, G. Baselli, M. G. Bruzzone, I. Zucca, G. Cavallo, G. Terraneo, F. Baldelli Bombelli, P. Metrangolo, G. Resnati, *Journal of the American Chemical Society* **2014**, *136*, 8524-8527; [c]M. Srinivas, P. Boehm-Sturm, C. G. Figdor, I. J. de Vries, M. Hoehn, *Biomaterials* **2012**, *33*, 8830-8840.

[8] A. T. Preslar, F. Tantakitti, K. Park, S. Zhang, S. I. Stupp, T. J. Meade, *ACS Nano* **2016**, *10*, 7376-7384.

[9] [a]M. Srinivas, A. Heerschap, E. T. Ahrens, C. G. Figdor, I. J. M. d. Vries, *Trends in Biotechnology* **2010**, *28*, 363-370; [b]S. Bo, Y. Yuan, Y. Chen, Z. Yang, S. Chen, X. Zhou, Z.-X. Jiang, *Chemical Communications* **2018**, *54*, 3875-3878; [c]E. Hequet, C. Henoumont, R. N. Muller, S. Laurent, *Future Medicinal Chemistry* **2019**, *11*, 1157-1175; [d]D. Jirak, A. Galisova, K. Kolouchova, D. Babuka, M. Hruby, *Magnetic Resonance Materials in Physics, Biology and Medicine* **2019**, *32*, 173-185; [e]C. Chirizzi, D. D. Battista, I. Tirotta, P. Metrangolo, G. Comi, F. B. Bombelli, L. Chaabane, *Radiology* **2019**, *291*, 351-357; [f]O. Koshkina, G. Lajoinie, F. Baldelli Bombelli, E. Swider, L. J. Cruz, P. B. White, R. Schweins, Y. Dolen, E. A. W. van Dinther, N. K. van Riessen, S. E. Rogers, R. Fokkink, I. K. Voets, E. R. H. van Eck, A. Heerschap, M. Versluis, C. L. de Korte, C. G. Figdor, I. J. M. de Vries, M. Srinivas, *Advanced Functional Materials* **2019**, *29*, 1806485; [g]S. D. C. Anne H. Schmieder, Jochen Keupp,Samuel A. Wickline,Gregory M. Lanza, *Engineering* **2015**, *1*, 475-489.

[10] [a]J. Wang, M. Sánchez-Roselló, J. L. Aceña, C. del Pozo, A. E. Sorochinsky, S. Fustero, V. A. Soloshonok, H. Liu, *Chemical Reviews* **2014**, *114*, 2432-2506; [b]Y. Zhou, J. Wang, Z. Gu, S. Wang, W. Zhu, J. L. Aceña, V. A. Soloshonok, K. Izawa, H. Liu, *Chemical Reviews* **2016**, *116*, 422-518.

[11] M. Cametti, B. Crousse, P. Metrangolo, R. Milani, G. Resnati, *Chemical Society Reviews* **2012**, *41*, 31-42.

[12] C. Pigliacelli, D. Maiolo, Nonappa, J. S. Haataja, H. Amenitsch, C. Michelet, P. Sánchez Moreno, I. Tirotta, P. Metrangolo, F. Baldelli Bombelli, *Angewandte Chemie International Edition* **2017**, *56*, 16186-16190.

[13] [a]J. Zhu, Y. Xiao, H. Zhang, Y. Li, Y. Yuan, Z. Yang, S. Chen, X. Zheng, X. Zhou, Z.-X. Jiang, *Biomacromolecules* **2019**, *20*, 1281-1287; [b]O. Sedlacek, D. Jirak, A. Galisova, E. Jager, J. E. Laaser, T. P. Lodge, P. Stepanek, M. Hruby, *Chemistry of Materials* **2018**, *30*, 4892-4896; [c]C. Fu, J. Tang, A. Pye, T. Liu, C. Zhang, X. Tan, F. Han, H. Peng, A. K. Whittaker, *Biomacromolecules* **2019**, *20*, 2043-2050; [d]A. Piloni, R. Simonutti, M. H. Stenzel, *Journal of Polymer Science Part A: Polymer Chemistry* **2019**, *57*, 1994-2001.

[14] [a]N. Bourouina, D. W. de Kort, F. J. M. Hoeben, H. M. Janssen, H. Van As, J. Hohlbein, J. P. M. van Duynhoven, J. M. Kleijn, *Langmuir* **2015**, *31*, 12635-12643; [b]V. Pourcelle, S. Laurent, A. Welle, N. Vriamont, D. Stanicki, L. Vander Elst, R. N. Muller, J. Marchand-Brynaert, *Bioconjugate Chemistry* **2015**, *26*, 822-829; [c]M. Zieringer, M. Wyszogrodzka, K. Biskup, R. Haag, *New Journal of Chemistry* **2012**, *36*, 402-406; [d]S. Li, Y. Yuan, Y. Yang, C. Li, M. T. McMahon, M. Liu, S. Chen, X. Zhou, *Journal of Materials Chemistry B* **2018**, *6*, 4293-4300; [e]C. Fu, B. Demir, S. Alcantara, V. Kumar, F. Han, H. G. Kelly, X. Tan, Y. Yu, W. Xu, J. Zhao, C. Zhang, H. Peng, C. Boyer, T. M. Woodruff, S. J. Kent, D. J. Searles, A. K. Whittaker, *Angewandte Chemie* **2020**, *n/a*.

[15] B. E. Rolfe, I. Blakey, O. Squires, H. Peng, N. R. B. Boase, C. Alexander, P. G. Parsons, G. M. Boyle, A. K. Whittaker, K. J. Thurecht, *Journal of the American Chemical Society* **2014**, *136*, 2413-2419.

[16] V. Dichiarante, M. I. Martinez Espinoza, L. Gazzera, M. Vuckovac, M. Latikka, G. Cavallo, G. Raffaini, R. Oropesa-Nuñez, C. Canale, S. Dante, S. Marras, R. Carzino, M. Prato, R. H. A. Ras, P. Metrangolo, *ACS Sustainable Chemistry & Engineering* **2018**, *6*, 9734-9743.

[17] L. Zhang, Y. Li, C. Zhang, Y. Wang, C. Song, *International journal of nanomedicine* **2009**, *4*, 175-183.

[18] D. S. Miron, C. Soldattelli, E. E. S. Schapoval, *Chromatographia* **2006**, *63*, 283-287.

[19] H. S. Yoo, T. G. Park, *Journal of Controlled Release* **2004**, *96*, 273-283.

[20] C. D'Avila Carvalho Erbetta, R. José Alves, J. Magalhães Resende, R. Fernando de Souza Freitas, R. G. d. Sousa, *Journal of Biomaterials and Nanobiotechnology* **2012**, *3*, 208-225.

[21] M. Boccalon, P. Franchi, M. Lucarini, J. J. Delgado, F. Sousa, F. Stellacci, I. Zucca, A. Scotti, R. Spreafico, P. Pengo, L. Pasquato, *Chemical Communications* **2013**, *49*, 8794-8796.

[22] C. Zhang, S. S. Moonshi, Y. Han, S. Puttick, H. Peng, B. J. A. Magoling, J. C. Reid, S. Bernardi, D. J. Searles, P. Král, A. K. Whittaker, *Macromolecules* **2017**, *50*, 5953-5963.

[23] J. M. Janjic, E. T. Ahrens, *Wiley Interdisciplinary Reviews: Nanomedicine and Nanobiotechnology* **2009**, *1*, 492-501.

[24] A. V. Fuchs, A. P. Bapat, G. J. Cowin, K. J. Thurecht, *Polymer Chemistry* **2017**, *8*, 5157-5166.

[25] [a]N. Hoshyar, S. Gray, H. Han, G. Bao, *Nanomedicine* **2016**, *11*, 673-692; [b]R. Bruni, P. Possenti, C. Bordignon, M. Li, S. Ordanini, P. Messa, M. P. Rastaldi, F. Cellesi, *Journal of Controlled Release* **2017**, *255*, 94-107.

[26] C. Colombo, M. Li, S. Watanabe, P. Messa, A. Edefonti, G. Montini, D. Moscatelli, M. P. Rastaldi, F. Cellesi, *ACS Omega* **2017**, *2*, 599-610.

[27] G. I. Welsh, M. A. Saleem, *Nature Reviews Nephrology* **2011**, *8*, 14.

[28] C. E. Mora-Huertas, H. Fessi, A. Elaissari, *International Journal of Pharmaceutics* **2010**, *385*, 113-142.

[29] aM. Chorny, I. Fishbein, H. D. Danenberg, G. Golomb, *Journal of Controlled Release* **2002**, *83*, 389-400; bF. Lince, D. L. Marchisio, A. A. Barresi, *Journal of Colloid and Interface Science* **2008**, *322*, 505-515.